JOURNAL OF AGRICULTURAL AND FOOD CHEMISTRY

Molecular Action Mechanism against Apoptosis by Aqueous Extract from Guava Budding Leaves Elucidated with Human Umbilical Vein Endothelial Cell (HUVEC) Model

CHIU-LAN HSIEH,*[,†,§] CHIEN-NING HUANG,[#] YUH-CHARN LIN,[§] AND ROBERT Y. PENG[§,⊥]

Department of Food and Nutrition, Research Institute of Biotechnology, Hungkuang University, 34 Chung-Chie Road, Shalu County, Taichung Hsien, Taiwan 43302; Division of Endocrinology and Metabolism, Department of Internal Medicine, Chung-Shan Medical University Hospital, Chung-Shan Medical University, 110 Chien-Kuo S. Road, Taichung City, Taiwan; and Research Institute of Medical Sciences, Taipei Medical University, Wu-Xin Street, Xin-Yi District, Taipei 110, Taiwan

Chronic cardiovascular and neurodegenerative complications induced by hyperglycemia have been considered to be associated most relevantly with endothelial cell damages (ECD). The protective effects of the aqueous extract of *Psidium guajava* L. budding leaves (PE) on the ECD in human umbilical vein endothelial cell (HUVEC) model were investigated. Results revealed that glyoxal (GO) and methylglyoxal (MGO) resulting from the glycative and autoxidative reactions of the high blood sugar glucose (G) evoked a huge production of ROS and NO, which in turn increased the production of peroxynitrite, combined with the activation of the nuclear factor κB (NFκB), leading to cell apoptosis. High plasma glucose activated p38-MAPK, and high GO increased the expressions of p38-MAPK and JNK-MAPK, whereas high MGO levels induced the activity of ERK-MAPK. Glucose and dicarbonyl compounds were all found to be good inducers of intracellular PKCs, which together with MAPK acted as the upstream triggering factor to activate NFκB. Conclusively, high plasma glucose together with dicarbonyl compounds can trigger the signaling pathways of MAPK and PKC and induce cell apoptosis through ROS and peroxynitrite stimulation and finally by NFκB activation. Such effects of PE were ascribed to its high plant polyphenolic (PPP) contents, the latter being potent ROS inhibitors capable of blocking the glycation of proteins, which otherwise could have brought forth severe detrimental effects to the cells.

KEYWORDS: ***Psidium guajava*** **L.; guava; apoptosis of HUVEC; MAPK; PKC; ROS; NFκB**

INTRODUCTION

Hyperglycemia is a casuality of chronic cardiovascular complications (*1*), whereas the endothelial cells are usually involved in a major role in this respect. Both the brain–blood barrier (BBB) and most parts of the cardiovascular system are composed of many thin and flat cells called endothelial cells, which line the small blood vessels (capillaries) of brain and circulation vessels. Under conditions of hyperglycemia, the relevant phenomenological changes associated with endothelial cells that had been observed included slowing of cell growth rate (*2*), significant extension of cell cycle (*3*), and apparently increased consumption of antioxidative substances (*4*), accompanied by more severe cell apoptosis (*5*, *6*). The literature has pointed out the major role of endothelial cells in chronic diabetic complications including atherosclerosis and neurodegenerations; hence, prevention of the detrimental effects has become the major research area of current pharmacology (*7*).

Glycation plays a major role in diabetic pathological changes (*8*). Long-term hyperglycemic status would facilitate glucose autoxidation, leading to glycation of proteins and formation of advanced glycation end products (AGEs), or simultaneously activate the polyol pathway, accelerating ROS production (*9*). Usually, activities of antioxidative enzymes SOD and catalase are lowered in diabetic patients with concomitant concentration declines of antioxidative biomolecules [e.g., glutathione (GSH), α-tocopherol, and L-ascorbic acid] (*10*). Conversely, serum levels of free radicals and lipid peroxides are significantly

* Address correspondence to this author at the Department of Food and Nutrition, Hungkuang University, 34 Chung-Chie Rd., Shalu County, Taichung Hsien, Taiwan 43302 (e-mail clhsieh@sunrise.hk.edu.tw; cell phone +886-2-921-753-069; telephone +886-4-26318652, ext., 5031; fax +886-2-27585767).

† Department of Food and Nutrition, Hungkuang University.

§ Research Institute of Biotechnology, Hungkuang University.

Chung-Shan Medical University.

⊥ Taipei Medical University.

10.1021/jf071858b CCC: $37.00
Published on Web 09/26/2007

elevated (*11*), forcing the diabetic patients to face more severe oxidative stress and damages. Subramaniam et al. (*12*) indicated that the AGEs resulting from the glycation of bovine serum albumin induced by GO and MGO had effected tremendous production of ROS in RAW 264.7 macrophage cells, more dominantly in the presence of Cu^{2+} ions. Even in the absence of Cu^{2+} ions and oxygen, direct cross-linking of alanine is initiated by MGO, resulting in the formation of the cross-linked radical and MGO radical cations, which on exposure to oxygen can release electrons leading to the formation of superoxide anions (*13*).

NFκB acts as the oxidative stress cellular sensor (*14*), playing an important target role in diabetic complications (*15*). Expressions of NFκB, PKC, and MAPK in HUVEC or smooth cells with hyperglycemia may always signal upstream cardiovasculopathy (*16*). Expressions of NFκB and nitric oxide synthase (NOS) in endothelial cells can be suppressed by superoxide dismutase (SOD) or antioxidants (*6*). Hyperglycemia usually initiates overproduction of superoxide anions through mitochondrial electron transport system (*17*), which in turn activates the activities of synthases involving both endothelial (*e*NOS) and inducible (*i*NOS) nitric oxide synthase to release more NO. As is well-known, interaction of both superoxide anions and NO produces the stronger oxidative chemical species peroxynitrite, which in turn causes DNA destruction and endothelial cell detriments (*18*), resulting in increased risks of diabetic cardiovascular complications.

Glycation of proteins usually is accompanied by huge production of ROS and free radicals (*19*). Accordingly, the use of antioxidants in the prevention of hyperglycemic complications, especially with respect to inhibition of AGEs formation, can be a promising strategy in treating diabetes (*20*). *Psidium guajava* L. (Myrtaceae), commonly called "guava", originated in Yuin-Nan, China, and Taiwan. Its leaf sap has long been used as an anti-inflammatory, antidiarrheal, psychic depressant remedy (*21*), and hypoglycemic (*22*). Oliver-Bever (*23*) identified three flavonoids in *P. guajava* leaves. Previously, we reported the presence of a profound content of polyphenolics in aqueous extracts of guava budding leaves (PE) and demonstrated its potent antiglycative bioactivity by LDL model induced by glucose, GO, and MGO (*24*). To determine whether PE could be also very potentially effective as a preventive against the oxidative detrimental effects occurring in endothelial cells, we further performed this investigation. Using this HUVEC model, we have successfully demonstrated potent antioxidative and antiglycative effects of PE against G, GO, and MGO. By examining the suppressive effects exerted by PE on the expressions of MAPK and PKC, NO release, and ROS production with subsequent NFκB expression, we elucidated a molecular action mechanism of PE acting as an antiapoptotic agent against the detrimental effects of hyperglycemia in the HUVEC model.

MATERIALS AND METHODS

Glucose (G), glyoxal (GO), methylglyoxal (MGO), aminoguanidine (AG), bovine serum albumin (BSA), NaN_3, sodium dodecyl sulfate (SDS), ethylene dinitrilotetraacetic acid (EDNTA) disodium salt dihydrate, trypsin-EDTA, 3-(4,5-dimethylthiazolyl-2)-2,5-diphenyltetrazolium bromide (MTT), dimethyl sulfoxide (DMSO), propidium iodide (PI), RNase, dichlorofluorescein (DCFH), dichlorofluorescin diacetate (DCFH-DA), sulfanilamide, *N*-1-naphthylethylenediamine (NED), Tris-HCl, glycerol, bromophenol blue, bis(*N*,*N*-methylenebisacrylamide), acrylamide, *N*,*N*,*N*′,*N*′-tetramethylethylenediamine (TEMED), tris-base, 2-mercaptoethanol (β-ME), Coomassie Brilliant Blue R (CBR), NP-40, sodium deoxycholate, phenylmethanesulfonyl fluoride, Na_3VO_4, NaF, aprotinin, proteinase inhibitor, Tween-20, hydrochloric acid (HCl), sodium chloride (NaCl), potassium chloride (KCl), potassium dihydrogen phosphate (KH_2PO_4), disodium hydrogen phosphate (Na_2HPO_4), and lactic dehydrogenase (LDH) assay kit were purchased from Sigma (St. Louis, MO). Ethanol and methanol were provided by E. Merck (Darmstadt, Germany). HUVEC and Medium 200 were supplied by Cascade Biologic Co. (Portland, OR). Protein assay reagents were supplied by Bio-Rad Co. (Hercules, CA). CNM compartment protein extraction kit was a product of BioChain Institute, Inc. (Hayward, CA). MAPK polyclonal antibodies, PKC polyclonal antibodies, and anti-mouse IgG were purchased from BD Biosciences Co. (Bedford, MA). NFκB assay kit was provided by Pierce Biotechnology Co. (Rockford, IL).

***P. guajava* L. Aqueous Extracts.** Desiccated guava budding leaves (1 part) were added with 10 parts of distilled water, refluxed at 100 °C for 30 min, and filtered through a Whatman no. 2 filter paper. Reflux was repeated three times, and the filtrates were combined and lyophilized. The percent yield was calculated according to

$$\% \text{ yield} = (W_e/W_L) \times 100$$

where W_L is the weight of desiccated guava budding leaves used and W_e is the weight yield of dried extract.

The product was kept at −20 °C for further use.

Characterization of Phenolic Compounds in Guava Leaves. Analyses were performed on a Finnigan Surveyor Modular HPLC system (Thermo Electron Co.). Chromatographic separation of the compounds was achieved using an analytical column, Luna 3 μm C18(2) 150 × 2.0 mm, and guard column, Security Guard C18 (ODS) 4 × 3.0 mm i.d. (Phenomenex, Inc., Torrance, CA), at a flow rate of 0.2 mL/min. Mobile phases A and B were water and acetonitrile, respectively, both containing 0.1% formic acid. Gradient elution was conducted as follows: 0–15 min, 5% B; 15–50 min, 5–40% B; and 50–55 min, 40–95% B, with a linear gradient, followed by 95% B at 55–65 min, isocratic. A photodiode array detector (PDA) was operated at wavelengths between 220 and 400 nm. The system was coupled to a Finnigan LCQ Advantage MAX ion trap mass spectrometer and operated in electrospray ionization (ESI) mode. The PE was re-extracted by acetone (1:5) and filtered through a 0.45 μm Micropore. Twenty microliters of the filtrate was directly injected into the column using a Rheodyne (model 7725i) injection valve. ESI source and negative ionization mode were used with different fragment voltages. Nitrogen was used as the neutralizing and drying gas. The typical operating parameters were as follows: spray needle voltage, 5 kV; ion transfer capillary temperature, 300 °C; nitrogen sheath gas, 40; and auxiliary gas, 5 (arbitrary units). The ion trap contained helium damping gas, which was introduced in accordance with the manufacturer's recommendations. Mass spectra were acquired in a *m*/*z* range of 100–1000, with five microscans and a maximum ion injection time of 200 ms. The SIM analysis was a narrow scan event that monitored the *m*/*z* value of the selected ion, in a range of 1.0 centered on the peak for the molecular ion; this function was used in the analysis of molecular ions of the phenolic compounds in extracts using negative ESI modes (*25*).

HPLC Identification. An analytical column [Luna 5 μ C18 (2), 250 × 4.6 mm, Phenomenex Co.] was used for the analysis of major components in PE. Samples (20 μL) of PE extracts, filtered though a 0.45 μm Micropore, were directly injected for analysis. The mobile phase consisted of solvent A (1.5% glacial acetic acid) and solvent B (acetonitrile) and was programmed in a gradient elution profile: starting with solvent A/B (40:60) from 0 to 20 min, with A/B (15:85) from 21 to 35 min, and then with A/B (30:70) from 45 min, all operated at flow rates of 1 mL/min. Absorbance was measured at 284 nm using a DAD. The PDAs were located and identified in the HPLC-UV patterns by comparing their retention times and UV (210–400 nm) spectra with those of authentic samples (A. G. Scientific, San Diego, CA).

Cell Culture. The culture medium used for cultivation of HUVEC was Medium 200 (with 2% fetal bovine serum, 1 μg/mL hydrocortisone, 10 ng/mL human epidermal growth factor, 3 ng/mL basic fibroblast growth factor, and 10 μg/mL heparin added); HUVEC were cultivated in an incubator at 37 °C under a 5% CO_2 atmosphere. Passages were

Table 1. Chromatographic and Selective Fragment Ions of Compounds Detected in Extracts of Guava Budding Leaves by LC/ESI-MS[a]

peak	retention time (min)	assigned identity	UV λ_{max} (nm)	$[M - H]^+$ *m/z*
1	6.52	gallic acid	270, 225	168.9
2	30.89	catechin	230, 229	289.1
3	36.44	epicatechin	230, 279	289.0
4	39.62	rutin	256, 354	609.2
5	50.53	quercetin	254, 370	301.1
6	54.59	naringenin	231, 288	271.1
7	55.56	kaempferol	367, 265	285.1

[a] Selective ion monitor of the $[M - H]^+$ in extracts of guava leaves. Samples of 20 μL of extracts, filtered through 0.45 μm Micropore, were directly injected into the column using a Rheodyne (model 7725i) injection valve.

continued with addition of 0.025% trypsin–0.01% EDTA; passages 4–7 were used in this experimentation.

MTT Assay. HUVEC (1×10^4 cells), plated onto a 24-well plate and treated with different drugs as indicated, were cultivated for 48 h. Cells were rinsed twice with PBS and added with the same culture medium containing 0.5 mL of MTT (0.5 mg/mL). Cultivation was continued for an additional 3.5 h at 37 °C. MTT containing medium was sucked off. The precipitated formazan was dissolved with the addition of DMSO (1 mL). Absorbance was read at 570 nm, and viability was calculated (*26*).

LDH Release Assay. The LDH release assay has been used as the cytotoxicity marker. HUVEC (1×10^4 cells) were plated onto a 24-well plate and incubated for 48 h after the addition of the target drugs. The LDH release was analyzed with a LDH kit (Sigma) by following the manufacturer's instructions. Briefly, the culture medium was centrifuged at 250*g* for 10 min; the supernatant (120 μL) was transferred into a 96-well plate, 60 μL of lactate dehydrogenase assay mixture (substrate/enzyme/dye solution = 1:1:1) was added, and the mixture was left to stand at ambient temperature for 30 min, avoiding direct light irradiation. Eighteen microliters of 1 N HCl was added to stop the reaction. Absorbance was read at 490 nm to determine the amount of LDH released (L_r). Alternatively, HUVEC were lysed using a cell lytic solution (50 mM Tris-HCl, pH 7.5; 150 mM NP-40; 0.25% sodium deoxycholate; 1 mM phenylmethanesulfonyl fluoride; 1 mM Na_3VO_4; 50 mM NaF; aprotinin, 10 μg/mL; 0.1% SDS; proteinase inhibitor) after the cultivation was finished. The lysed solution was centrifuged at 250*g*. Supernatant was measured similarly for LDH activity to obtain the total LDH (L_t). The percent LDH released was calculated using

$$\% \text{ LDH released} = (L_r/L_t) \times 100$$

Cell Cycle Analysis. The HUVEC, after treatment with PE, G, GO, and MGO for a certain length of time as indicated, were treated with PI stain according to the method of Takada et al. (*27*). Briefly, the incubated culture medium was first sucked out, and the cells were rinsed twice with PBS and reacted with 0.5 mL of trypsin-EDTA solution for 1–2 min. Finally, the reaction was terminated with 1 mL of medium. The adhered cells were detached from the dish and subjected to centrifugation at 1500 rpm for 10 min. The sedimented cells were collected and rinsed twice with PBS and treated with 1 mL of ethanol (80%) to generate pores on the cell membranes to facilitate the PI staining. The cells were stored at −20 °C for at least 30 min and then centrifuged at 1500 rpm for 10 min to collect the cell sediments. The sediments were rinsed twice again with PBS and transferred into an Eppendorf tube. To each tube was added 0.1 mg/mL RNase plus 40 μg/mL PI (aliquots of 100 μL from 10 mg/mL RNase; and 40 μg of solution of 400 μg of PI in 10 mL of PBS), and the tubes were kept in the dark for 15 min to facilitate the reaction. The DNA content was measured with flow cytometry.

Expression of MAPK. The HUVEC, after treatment with PE, G, GO, and MGO for 48 h, were completely lysed using cell lytic solution (50 mM Tris-HCl, pH 7.5; 150 mM NP-40; 0.25% sodium deoxycholate; 1 mM phenylmethanesulfonyl fluoride; 1 mM Na_3VO_4; 50 mM NaF; aprotinin, 10 μg/mL; 0.1% SDS; proteinase inhibitor). The lysed mixture was centrifuged. The protein content of the supernatant was determined with the protein assay kit. In parallel, the same amount of protein was measured and dispensed to make up the same volume. On addition of the reducing buffer, the mixture was heated at 95 °C for 5 min. The resulting solution was run on a 10% SDS-PAGE. The gel was removed, and the proteins were mounted on the nitrocellulose membrane (NCM). The NCM was soaked in a soaking solution PBST (containing 5% skimmed milk and 0.2% Tween-20, pH 7.4) for 1 h. The MAPK polyclonal antibodies were added and mixed with gentle agitation for 1 h. The NCM was rinsed with PBST four times, each time for 15 min. The PBST washings were decanted. The residue NCM was soaked in the secondary antibodies-containing PBST with gentle agitation for an additional 1 h and rinsed again four times with PBST, each time for 15 min. Finally, the assay was carried out using the ECL Supersignal substrate to serve as the substrate.

Expression of PKC. The HUVEC, after treatment with PE, G, GO, and MGO for 48 h, were extracted with CNM compartment protein extraction kit (BioChain Institute, Inc.) to obtain the membrane proteins. The protein contents were assayed using a protein assay kit. In parallel, the same amount of protein was measured and dissolved to make the same volume. On addition of the reducing buffer, the mixture was heated at 95 °C for 5 min. The resulting solution was run on a 10% SDS-PAGE. The gel was removed, and the proteins were mounted on the nitrocellulose membrane (NCM). The NCM was soaked in a soaking solution of PBST (containing 5% skimmed milk and 0.2% Tween-20, pH 7.4) for 1 h. The PKC polyclonal antibodies were added and mixed with gentle agitation for 1 h. The NCM was rinsed with PBST four times, each time for 15 min. The PBST washings were decanted, and the NCM was added with the secondary antibodies-containing PBST, mixed with gentle agitation for an additional 1 h, and finally assayed with the Western-Star Chemiluminescence Detection System using ECL Supersignal substrate to serve as the substrate.

Expression of NFκB. The HUVEC, after treatment with PE, G, GO, and MGO for 48 h, were extracted with CNM compartment protein extraction kit (BioChain Institute, Inc.) to obtain the membrane proteins. The protein contents were assayed using a protein assay kit. The same amount of protein was measured and dispensed into the same volume. The protein analyses were proceeded with the Transcription Factor Kits for p65 (Pierce Biotechnology). In a 96-well plate, 50 μL of working buffer with nuclear protein solutions was added and the reaction allowed to proceed at ambient temperature for 1 h, followed by three rinses with wash buffer (200 μL); 100 μL of primary antibody was added and allowed to react for 1 h, followed again by three rinses with wash buffer (200 μL). Finally, 100 μL of substrate working solution (Luminol/Enhancer solution/stable peroxide solution = 1:1) was added, and the intensity of cold light was measured with a luminescence cold light detector using the TNFα activated HeLa cell nuclear extract as the positive control.

ROS Quantification. The procedure was performed according to that of Pan et al. (*28*). Dichlorodihydrofluorescein diacetate (DCFH-DA) was used for determination of the intracellular ROS production. In principle, DCFH-DA is able to readily penetrate the cell membrane, whereas the diacetate esteric form can be rapidly de-esterified by the membrane-bound enzyme esterase to yield DCFH free form, which is the reduced form of the fluorescent dichlorofluorescein (DCF). On reaction with ROS, DCFH is oxidized to yield the fluorescent DCF; thus, the intensity of the fluorescence can be correlated with the amount of ROS formed in situ. Briefly, HUVEC (4×10^5 cells) were cultivated in a 6 cm dish, treated with different drug preparations as indicated; after the cultivated medium had been sucked out, the cells were rinsed with PBS twice, treated with 0.5 mL of trypsin–EDTA solution for 1–2 min, and terminated with 1 mL of medium. The adhered cells were detached from the dish and centrifuged at 1500 rpm for 10 min. The sedimented cells were collected, and 1 mL of PBS and 1 μL of 20 mM DCFH-DA were added to make a final concentration of 20 μM. The mixture was incubated at 37 °C for 30 min and centrifuged at 1500 rpm for 10 min to collect the sedimented cells. On resuspension of the cells with 0.5 mL of PBS, the flow cytometic analysis was performed.

NO Release. HUVEC (1×10^4 cells) were plated onto a 24-well plate and treated with different drug preparations for 24 h as indicated. The method decribed by Eu et al. (*29*) was followed. Briefly, aliquots of 50 μL were transferred into a 96-well microplate; to each well 50 μL of sulfanilamide solution (1%) was added and allowed to react for

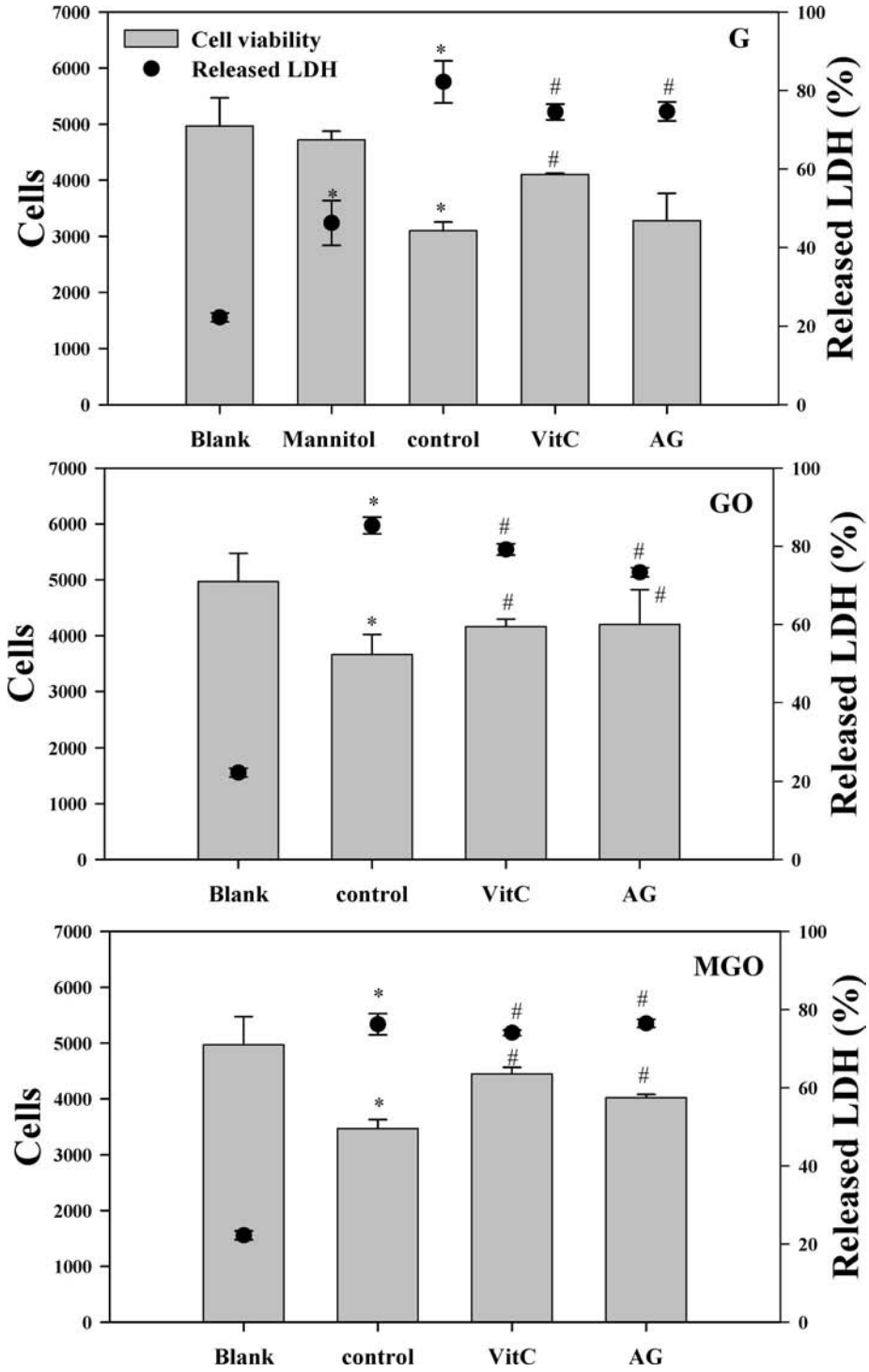

Figure 1. Effects of G, GO, and MGO on cell viability and LDH release in HUVEC. HUVEC was incubated with G (30 mM), GO, and/or MGO (0.5 mM) at 37 °C for 2 days in the absence and presence of VitC (50 μM) or AG (50 μM). Data are expressed as mean ± SD from triplicate experiments. ∗, $p < 0.05$ compared with blank; #, $p < 0.05$ compared with control.

10 min while avoiding direct light exposure. On addition of *N*-1-naphthylethylenediamine (NED) solution (NED 0.1%, 50 μL) and standing in the dark for another 10 min, the absorbance was read at 550 nm.

RESULTS AND DISCUSSION

PE Contains Seven Main Constituents. Seven major components in PE were identified by LC/ESI-MS. The physical data assigned were as follows: gallic acid, retention time t_R = 6.52 min, $[M - H]^+$ *m/z* 168.9; catechin, t_R = 30.89 min, $[M - H]^+$ *m/z* 289.1; epicatechin, t_R = 36.44 min, $[M - H]^+$ *m/z* 289.0; ruitn, t_R = 39.62 min, $[M - H]^+$ *m/z* 609.2; quercetin, t_R = 50.53 min, $[M - H]^+$ *m/z* 301.1; naringenin, t_R = 54.59 min, $[M - H]^+$ *m/z* 271.1; and kaempferol, t_R = 55.56 min, $[M - H]^+$ *m/z* 285.1 (**Table 1**). In the secondary methanolic extract from PE, we found the content of each constituent was as follows: gallic acid, 86 mg/g; catechin, 132 mg/g; epicatechin, 60 mg/g; rutin, 110 mg/g; and quercetin, 56 mg/g. Naringenin and kaempferol were present in only trace amounts (data not shown). Previously, Hsieh et al. (*24*) reported PE contained very high polyphenolic content, reaching a gallic equivalent of 165.61 mg/g (*24*). Both polyphenolics and flavonoids are excellent free

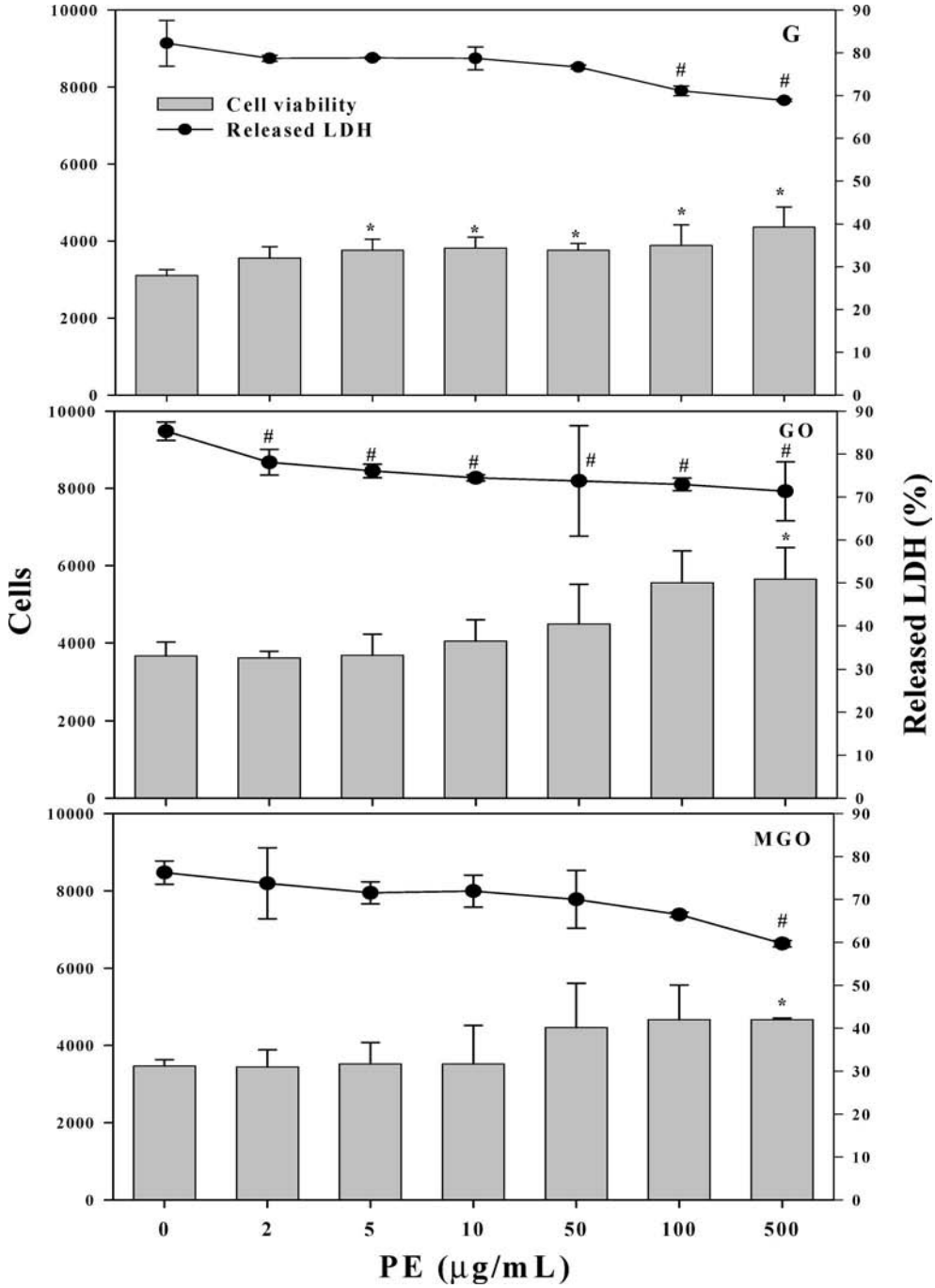

Figure 2. Effect of PE on cell viability and LDH release in HUVEC induced by glucose, glyoxal, and methylglyoxal. HUVEC was incubated with G (30 mM), GO, and/or MGO (0.5 mM) at 37 °C for 2 days in the absence and presence of PE (0–0.1 mg/mL). Data are expressed as mean ± SD from triplicate experiments. ∗, $p < 0.05$ compared with PE 0 mg/mL.

radical scavengers as well as ferrous ion chelators (*30*). Quercetin in vivo as well as in vitro is a good antiglycative biochemical capable of inhibiting diabetic complications (*31*), preventing the in vivo oxidative β-cell damages caused by streptozotocin (*32*) and neurodetrimental effects (*33*). Similar effects were found for ferulic acid associated with glycation of aspartate aminotransferase model induced by D-fructose (*34*), and also for gallate as well (*35*), implying that the prevailing wide spectrum of antiglycative and antiapoptotic bioactivities of PE can be attributed to these major constituents. Clinically, supplements with antioxidants to inhibit the AGEs production now have been adopted as the new strategy for delaying aging, neurodegeneration, and diabetic complications.

Cell Viability: MTT Assay. Cell viabilities of HUVEC affected by G (30 mM) and the dicarbonyls GO (0. 5 mM) and MGO (0.5 mM) were examined in parallel with LDH release. Using mannitol as the reference osmotic control, the cell detrimental effects in HUVEC were compared. As a contrast, L-ascorbic acid and AG were used as the positive controls. As can be found, cell viabilities were suppressed to 62.46, 73.68, and 69.82% ($p < 0.05$) by G, GO, and MGO, respectively (**Figure 1**). LDH release was increased to 82.22, 85.32, and 76.23% ($p < 0.05$), respectively, compared with the control (22.22%). Apparently osmotic effect (mannitol osmosis control) (**Figure 1**) did not exert any significant effect on cell viability, evidencing direct apoptotic effects exerted by these inducers.

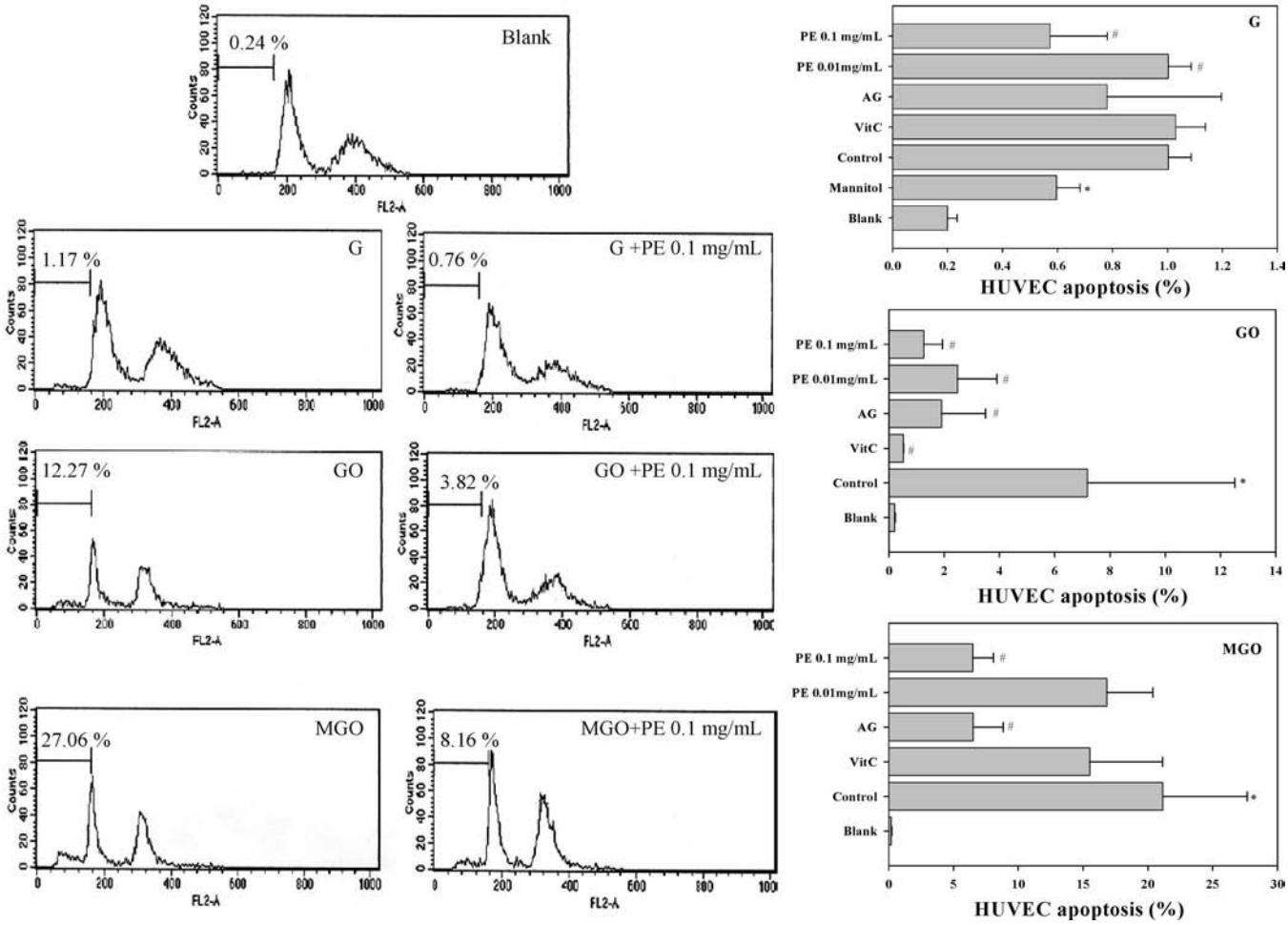

Figure 3. Effect of PE on cell apoptosis in HUVEC induced by glucose, glyoxal, and methylglyoxal. HUVEC was incubated with G (30 mM), GO, and/or MGO (0.5 mM) at 37 °C for 2 days in the absence and presence of PE (0–0.5 mg/mL). Data are expressed as mean ± SD from triplicate experiments. ∗, $p < 0.05$ compared with blank; #, $p < 0.05$ compared with control.

As found in **Figure 1**, the amount of LDH release was inversely related with the cell viability. Apparently, L-ascorbic acid (50 μM) was superior to aminoguanine (50 μM) in saving the HUVEC viability when damaged by G and MGO (**Figure 1**), yet only comparable effects were observed for GO category, implying different molecular mechanisms exerted by PE against these inducers. On the basis of the results obtained from cell viability assay (**Figures 1** and **2**) and, moreover, with the speculation that PE contains gallic acid, catechin, epicatechin, rutin, and quercetin from 56 to 132 mg/g, whether these polyphenolics could be wholly responsible for the bioactivity of PE, we performed tests using these compounds both separately and mixed on the HUVEC model system to determine which one could be the active principle in PE. All polyphenolics present in PE showed comparable potency in cell viability protection, ranging from 68.9% for rutin to 73.8% for catechin at 50 μM for each. In contrast, the mixed form of each individual component in similar proportions as in PE revealed a cell viability of 72.8% compared to 81.6% of PE (data not published). We ascribed such a discrepancy (8.8%) to the polysaccharide content in PE, which accounted for 5.43% in desiccated PE with an average molecular mass of 5029 kDa (data not published).

LDH Release versus Cell Viability. When PE at concentrations of 2–500 μg/mL was tested for cytotoxicity protective effect (**Figure 2**), significant protective effects of PE in category G were found in doses ranging from 5 to 500 μg/mL, whereas those affected by GO and MGO were observed only at 500 μg/mL PE (**Figure 2**). As shown in **Figure 2**, PE at a concentration of 5 μg/mL, saved viability of HUVEC from 62.46% (negative control) to 75.71% in the presence of inducer G. Whereas at the same dose viabilities induced by GO and MGO were totally unaffected, protective effects were seen only at higher concentration (**Figure 2**). At concentrations of 50 and 100 μg/mL, PE saved the viability of HUVEC to 69.82% and 73.68% damaged by GO and to 99.60% and 93.92% damaged by MGO, respectively (**Figure 2**).

Hyperglycemic status can induce elevated ROS and superoxide anion production in HUVEC through the action of glucose and the intermediate dicarbonyl inducers GO and MGO produced through autoxidation of glucose, activating the activity of NOS, resulting in the formation of intracellular peroxynitrite; the latter is a very potent oxidative agent capable of damaging intracellular DNA, eventually inducing cell apoptosis (refer to **Figure 9**). In **Figure 2**, PE at concentrations between 2 and 500 μg/mL was seen to have effectively inhibited the LDH releases induced by G (30 mM), GO (0.5 mM), and MGO (0.5 mM). Initial LDH releases (82.22, 85.32, and 76.23%) were suppressed to 76.67, 78.32, and 66.46%, respectively, by PE at 50 μg/mL (**Figure 2**). However, significant inhibitions were found only at 100 μg/mL by G, at concentrations higher than 2 μg/mL by GO, and at much higher dosage of 500 μg/mL by MGO (**Figure 2**). The increase in LDH release confirmed membrane perturbation and a loss of membrane integrity (*36*). PE moderately inhibited LDH release; protective effect was only 5.55, 7.00, and 9.77% against induction by G, GO, and MGO,

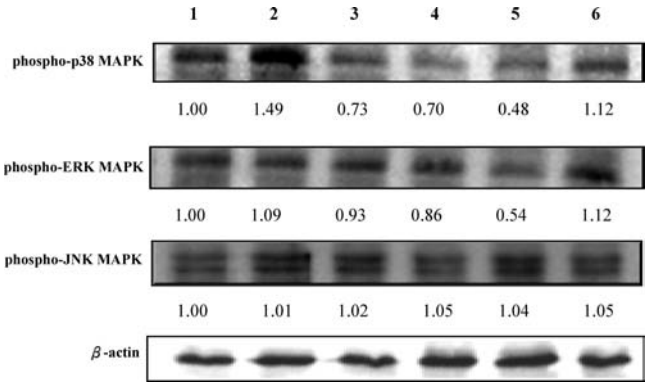

Figure 4. Effect of PE on MAPK expression in HUVEC induced by glucose. HUVEC was incubated with G (30 mM) at 37 °C for 3 days in the absence or presence of PE (0.1 mg/mL), L-ascorbic acid (50 μM), or AG (50 μM). Lanes: 1, blank; 2, 30 mM G; 3, 23 mM mannitol; 4, 30 mM G + PE 0.1 mg/mL; 5, 30 mM G + AG 50 μM; 6, 30 mM G + VitC 50 μM.

respectively. Decreased LDH release reflected increase in cell viability (**Figure 2**). As far as cell viability was concerned, PE most potently rescued cell viability in category GO and was least potent in G. Speculatively, different inducers exert different molecular action mechanisms.

HUVEC Cycle Analysis. From the above results, PE has been shown to be a good protectant capable of retarding the cell detrimental effects exerted by inducers as indicated. To further confirm the protective effect of PE against the apoptotic effect that might be caused by these inducers, flow cytometric analysis was performed using PI staining. As found in **Figure 3**, the apoptotic populations (0.24% as the control) were increased to 1.17, 12.27, and 27.06% when induced by G (30 mM), GO (0.5 mM), and MGO (0.5 mM), respectively ($p < 0.05$), which were significantly reduced by PE at 100 μg/mL (flow cytometric charts on the left-hand side in **Figure 3**) to 0.76, 3.82, and 8.16%, respectively (the right-hand side bar diagrams in **Figure 3**). Results again pointed out that PE suppressed apoptosis caused by different inducers by different molecular action mechanisms.

Current reports indicate high plasma glucose (G) levels induce apoptosis of HUVEC (*5*–*7*) by increasing osmotic permeabilty (*37*) and oxidative damages to DNA (*38*). Dicarbonyl compounds, glyoxal and methylglyoxal, resulting from protein glycation and glucose autoxidation (*39*), are also capable of inducing significant endothelial apoptosis (*38*). Such apoptotic phenomena were closely associated with intracellular ROS production (*38*). Which signal transduction pathway was involved? Now, the question is, which molecular mechanism mediated by PE was involved in the suppression of LDH release and apoptosis in HUVEC caused by these inducers?

PE Inhibited MAPK Activity. As can be seen, glucose (30 mM) significantly activated phospho-p38-MAPK compared to the control, mannitol (23 mM), which was significantly inhibited by treatment with PE at 100 μg/mL. Similar effects were found for positive controls AG and L-ascorbic acid (**Figure 4**), however unlikely for phospho-ERK-MAPK and phospho-JNK-MAPK (**Figure 4**). In contrast, GO (0.5 mM) significantly activated phospho-p38-MAPK (lane 2 of the first row in **Figure 5**) and moderately activated phospho-ERK-MAPK (lane 3 of the second row in **Figure 5**). MGO (0.5 mM) could activate only phospho-ERK-MAPK (lane 3 of the second row in **Figure 5**). Comparatively, both GO and MGO had no effect on phospho-JNK-MAPK (third row in **Figure 5**). Interestingly, activation of phospho-p38-MAPK by GO could be significantly inhibited

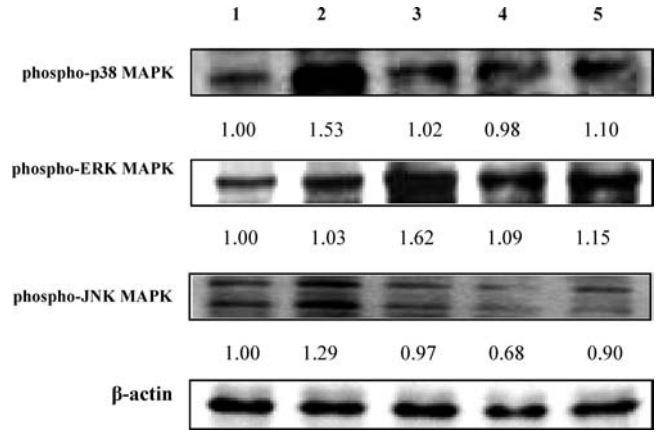

Figure 5. Effect of PE on MAPK expression in HUVEC induced by glyoxal and methylglyoxal. HUVEC was incubated with GO and/or MGO (0.5 mM) at 37 °C for 3 days in the absence and presence of PE (0.1 mg/mL). Lanes: 1, blank; 2, 0.5 mM GO; 3, 0.5 mM MGO; 4, 0.5 mM GO + PE 0.1 mg/mL; 5, 0.5 mM MGO + PE 0.1 mg/mL.

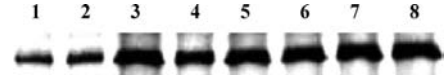

Figure 6. Effect of PE on various PKC expressions induced in HUVEC. HUVEC was incubated with G (30 mM), GO, and/or MGO (0.5 mM) at 37 °C for 3 days in the presence and absence of PE (0.1 mg/mL). Lanes: 1, blank; 2, 23 mM mannitol; 3, 30 mM G; 4, 0.5 mM GO; 5, 0.5 mM MGO; 6, 30 mM G + PE 0.1 mg/mL; 7, 0.5 mM GO + PE 0.1 mg/mL; 8, 0.5 mM MGO + PE 0.1 mg/mL.

by PE at 100 μg/mL (lanes 4 and 5 of the first row in **Figure 5**), yet activation of phospho-ERK-MAPK by GO and MGO was unaffected by PE at 100 μg/mL (lanes 4 and 5 of the second row in **Figure 5**). Over 15 years, there has been a dramatic increase in interest in the role of signaling pathways in governing neoplastic cell behaviors. Much of this interest has focused on members of the MAPK pathways, which include the ERK, the JNK, also called the SAPK, and the p38 kinase modules. Such signaling pathways regulate multiple biological activities, including cell proliferation, differentiation, cell cycle transverse, and survival, among others. Although exceptions occur, the bulk of evidence suggests that activation of the ERK (MAPK) pathway increases, in an unknown way, the cell death threshold; conversely, activations of JNK/SAPK and p38 kinase cascades are generally (although not universally) associated with enhanced activation of the apoptotic program. A corollary of some hypothetical models is that interruption of putatively cytoprotective signaling pathways in malignant cells could shift the balance away from survival toward cell death (*40*).

PE Significantly Inhibited PKC Activity. All of the inducers (G, 30 mM; GO, 0.5 mM; and MGO, 0.5 mM) were capable of activating PKC in HUVEC, among which only the PKC expression induced by G (30 mM) could be inhibited to slight extent by PE at 100 μg/mL (**Figure 6**).

MAPK and PKC all are upstream factors related to the apoptosis induced by G, GO, and MGO (*16*, *41*). Additionally, PKC can be activated by diacylglycerol (DAG), whereas in a hyperglycemic status, more DAG can be synthesized, which in turn can activate PKC, as often can be found in diabetic animal blood vessels, cornea, and glomerules (*17*), implying that activation of PKC (**Figure 6**) under hyperglycemic condition is also closely related with the elevated ROS production (**Figure**).

PE Apparently Inhibited ROS Production. The DCFH-DA fluorescence method revealed ROS production was actively

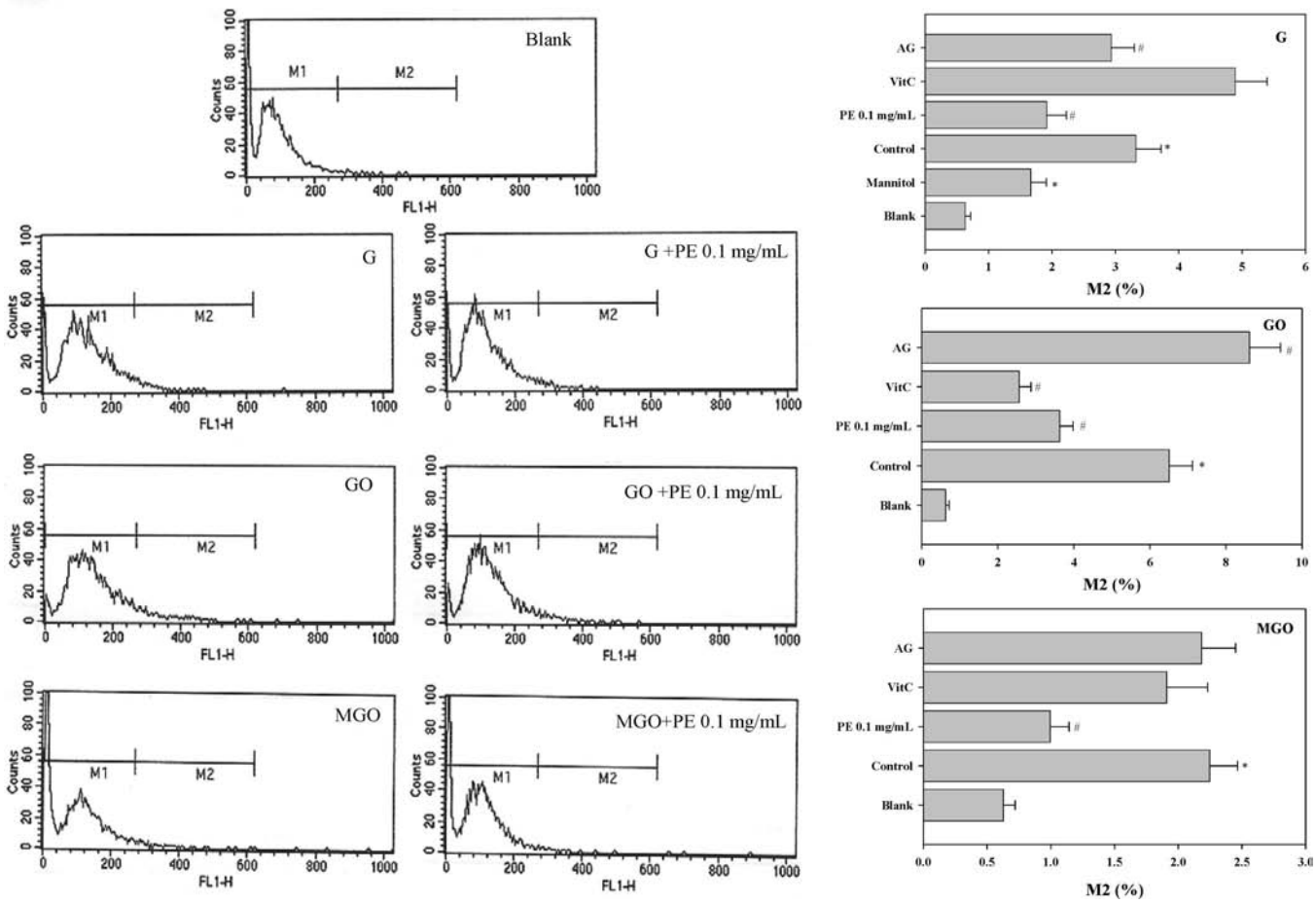

Figure 7. Effect of PE on ROS production in HUVEC induced by G, GO, and MGO measured by DCFH-DA fluorescence method. HUVEC was incubated with G (30 mM), GO (0.5 mM), and MGO (0.5 mM) at 37 °C for 1 day in the presence and absence of PE (0.1 mg/mL). ∗, $p < 0.05$ compared with blank; #, $p < 0.05$ compared with control.

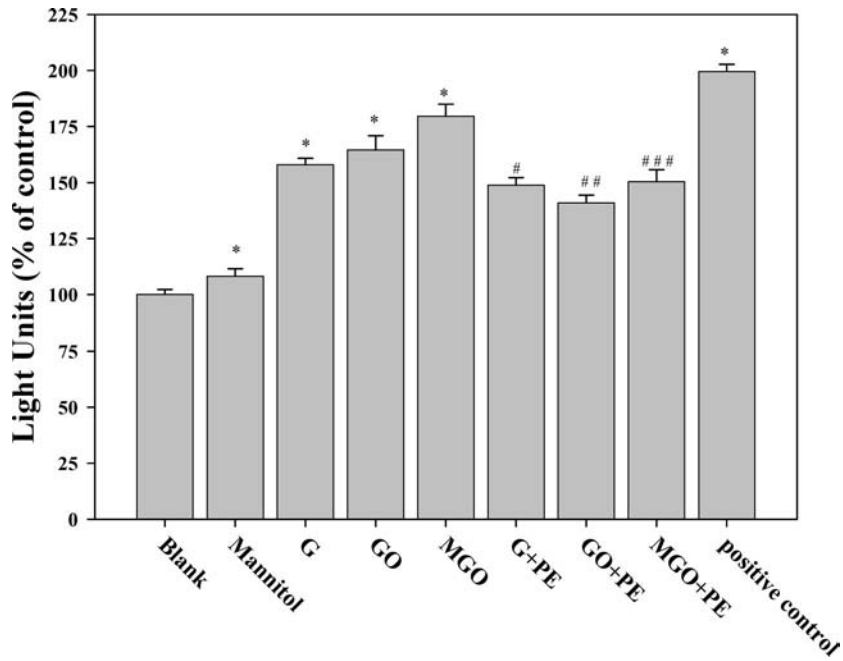

Figure 8. Effect of PE on various NFκB activations in HUVEC. HUVEC was incubated with G (30 mM), GO, and/or MGO (0.5 mM) at 37 °C for 2 days in the presence and absence of PE (0.1 mg/mL). Data are expressed as mean ± SD from triplicate experiments. Positive control: TNFα activated HeLa cell nuclear extract. ∗, $p < 0.05$ compared with blank; #, $p < 0.05$ compared with G; ##, $p < 0.05$ compared with GO; ###, $p < 0.05$ compared with MGO.

induced by the inducers G (30 mM), GO (0.5 mM), and MGO (0.5 mm). For comparison, the flow cytometric chart was divided into two parts: M1 and M2. As can be seen, ROS production caused the shift of part M2 farther to the right-hand side.

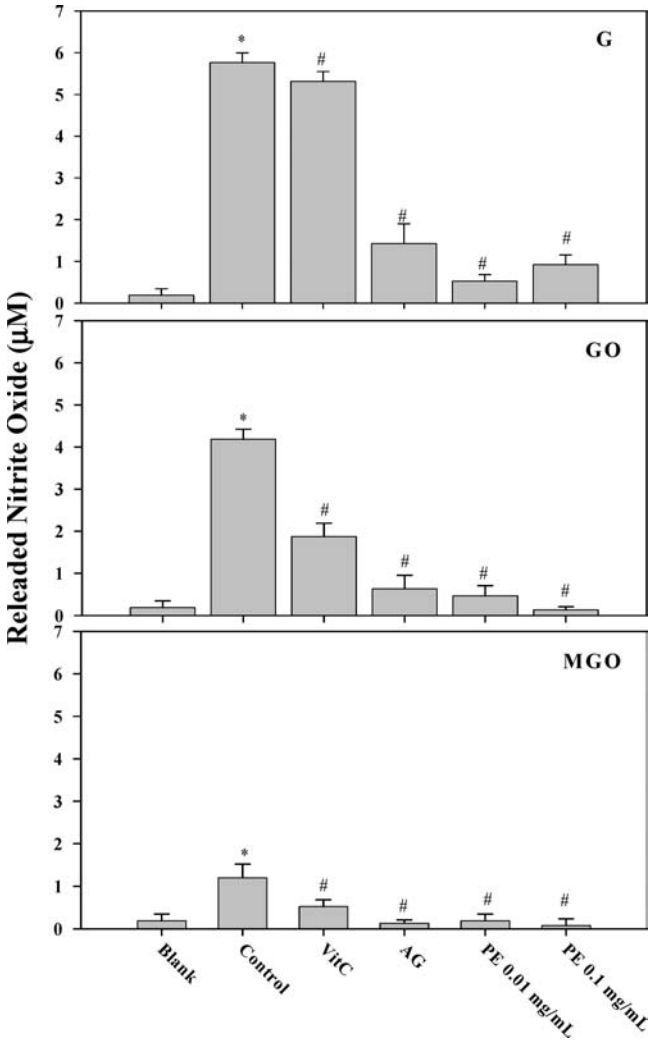

Figure 9. Effect of PE on NO release in HUVEC induced by G, GO, and MGO. HUVEC was incubated with G (30 mM), GO, and/or MGO (0.5 mM) at 37 °C for 1 day in the presence and absence of PE (0.01–0.1 mg/mL), VitC (0.05 mg/mL), or AG (0.05 mg/mL). Data are expressed as mean ± SD from triplicate experiments. ∗, $p < 0.05$ compared with blank; #, $p < 0.05$ compared with control.

Initially, part M2 increased from 0.63% (control) to 3.32, 6.51, and 2.25% ($p < 0.05$), respectively, resulting from induction by G, GO, and MGO (left column in **Figure 7**), whereas PE effectively and significantly suppressed those areas back to 1.92, 3.63, and 1.00% (central and right columns in **Figure 7**), respectively ($p < 0.05$).

PE Significantly Suppressed Expression of NFκB. Up-regulation of NFκB in HUVEC was significantly activated by G (30 mM), GO (0.5 mM), and MGO (0.5 mM) to 1.58-, 1.64-, and 1.80-fold, respectively, compared to the control (taken as a base = 1.00) ($p < 0.05$) (**Figure 8**). However, PE at 100 μg/mL showed significant inhibitory activity on these effects. The nuclear factor NFκB, which is reduction potential-sensitive, can be activated under conditions of hyperglycemia (*14*, *15*).

PE Effectively Suppressed NO Release from HUVEC. As shown in **Figure 9**, NO releases (5.76, 4.18, and 1.20 μM) from HUVEC were significantly increased when effected by incubation with G (30 mM), GO (0.5 mm), and MGO (0.5 mM), respectively (**Figure 9**) compared to the control (0.19 μM) ($p < 0.05$), which were suppressed to 0.52, 0.47, and 0.19 μM, respectively, on treatment with PE (10 μg/mL).

Recent research has focused on the superoxide anions produced in mitochondrial electron transport when induced by high plasma glucose and dicarbonyl inducer levels. Superoxide anions activate readily NO synthase in endothelial cells and hence indirectly enhance NO release, leading to higher risk of potent oxidative peroxynitrite formation. The latter, an active destructor of DNA, plays an important role in apoptosis induced in hyperglycemic patients (*6*, *42*).

Du et al. (*6*) pointed out that ROS formation in endothelial cell culture precedes the activation of NFκB as well as cell apoptosis; hence, antioxidants such as thiotic acid, α-tocopherol, and L-*N*-nitroarginine are reasonably able to block ROS damage. Wu et al. (*5*) demonstrated that ROS was actively produced in the first 24 h when incubated with a high glucose concentration, followed by apoptosis that occurred until 48 h postincubation, and more prominent apoptotic phenomenon was observed after 72 h. Consequently, antioxidants such as glutathione (GSH) and *N*-acetylcysteine were all effective inhibitors, similarly being consistent with the results obtained in this study.

ROS are very relevantly important activator for NFκB; both ROS and NFκB can lead to cell apoptosis. High glucose levels can induce p38-MAPK (**Figure 4**), high GO levels can up-regulate p38-MAPK and JNK-MAPK (**Figure 5**), and high MGO levels can induce ERK-MAPK (**Figure 5**). As mentioned, in the secondary methanolic extract from PE, we found the contents to be gallic acid, 86 mg/g; catechin, 132 mg/g; epicatechin, 60 mg/g; rutin, 110 mg/g; and quercetin, 56 mg/g [data not published; also refer to Hsieh et al. (*24*)]. With an aim to prevent detrimental effects on the LDL moiety of endothelial cells caused by ROS and AGEs, we used an aqueous extract of *P. guajava* budding leaves (PE), a high polyphenolics-containing preparation (*24*), to carry out this experimentation.

ROS (**Figure 7**) and NO (**Figure 9**) were actively produced in the first 24 h when HUVEC were incubated with high concentrations of glucose and dicarbonyl compounds, whereas with the activation of NFκB (**Figure 8**) the apoptosis and the up-regulations of the related signaling pathways (MAPK and PKC) (**Figures 46**) occurred only after incubation for 48 h. Such events can be readily inhibited by ascorbic acid (**Figure 3**), evidencing the existing high level of peroxynitrite derived from interaction of NO (**Figure 9**) with high levels of ROS (**Figure 7**) and superoxide anions to be the main cause of apoptosis (**Figure 3**). Moreover, aminoguanine (AG) was reported to be capable of effectively inhibiting all of the related signaling pathways (*2*, *3*, *6*). Evidence revealed a positive correlation between the apoptosis of HUVEC and the AGEs formed through glycation of proteins. Thus, speculatively, both ROS and AGEs can be the two killer factors for endothelial cells under hyperglycemic status.

Moreover, AGE receptor (RAGE) is also closely related with the activation of NFκB, which can result in modification of certain gene expressions (*17*). When glycated proteins combine with the RAGE on macrophages, ROS is produced thereby, evidencing that activation of NFκB is closely related with the oxidative stress. Whereas p38-MAPK and JNK-MAPK are the upstream factors of NFκB, MAPK (such as p38-MAPK and JNK-MAPK) is closely associated with the activity of NFκB. Activation of NFκB stimulates the production of inflammatory proteins such as tumor necrosis factor-α (TNF-α) and interleukin-1β (IL-1β), which in turn activate the expression of MAPK. Such a synergistic cycling effect may greatly enhance ROS production and exert more severe damages to endothelial cell (*6*).

To summarize, (1) PE is able to save HUVEC cell viability decrease caused by high plasma glucose and dicarbonyl inducer levels; (2) PE is capable of inhibiting the activation of p38-

MAPK and PKC induced by glucose, the expression of p38-MAPK induced by GO, and the activation of ERK-MAPK induced by MGO, leading to a promising antiapoptotic effect in HUVEC; (3) PE is capable of suppressing ROS production and NO release in HUVEC induced by high glucose and dicarbonyl inducer levels; (4) PE is capable of inhibiting the expression of NFκB in HUVEC induced by the high glucose and dicarbonyl inducer levels. The major part of bioactivity was exerted by polyphenolics, whereas other parts of bioactivity could be attributed to the polysaccharide (a peptidoglycan) content in PE. Conclusively, PE could be an effective antiapoptotic herbal preparation against cytotoxicity induced by glucose, glyoxal, and methylglyoxal, which is usually encountered in diabetic patients.

ABBREVIATIONS USED

ECD, endothelial cell damages; PE, *Psidium guajava* L. budding leaves; HUVEC, human umbilical vein endothelial cell; GO, glyoxal; MGO, methylglyoxal; G, glucose; ROS, reactive oxygen species; NO, nitric oxide; NFκB, nuclear factor κB; MAPK, P38-mitogen-activated protein kinase; JNK, JunN-terminal kinase; ERK, extracellular signal-regulated protein kinase; PKC, protein kinase C; PPP, plant polyphenolic; BBB, brain–blood barrier; AGEs, advanced glycation end products; SOD, superoxide dismutase; GSH, glutathione; NOS, nitric oxide synthase; eNOS, endothelial nitric oxide synthase; iNOS, inducible nitric oxide synthase; LDL, low-density lipoprotein; AG, aminoguanidine; LDH, lactic dehydrogenase; MTT, 3-(4,5-dimethylthiazolyl-2)-2,5-diphenyltetrazolium bromide; SAPK, stress-activated protein kinase; DAG, diacyl glycerol; DCFH-DA, 2′,7′-dichlorofluorescin diacetate; TNF-α, tumor necrosis factor-α; IL-1β, interleukin-1β.

LITERATURE CITED

(1) Goldberg, R. B.; Mellies, M. J.; Sacks, F. M.; Moye, L. A.; Howard, B. V.; Howard, W. J.; Davis, B. R.; Cole, T. G.; Pfeffer, M. A.; Braunwald, E. Cardiovascular events and their reduction with pravastatin in diabetic and glucose-intolerant myocardial infarction survivors with average cholesterol levels: subgroup analyses in the cholesterol and recurrent events (CARE) trial. *J. Am. Heart Assoc.* **1998**, *98*, 2513–2519.

(2) Rojas, S.; Rojas, R.; Lamperti, L.; Casanello, P.; Sobrevia, L. Hyperglycaemia inhibits thymidine incorporation and cell growth via protein kinase C, mitogen-activated protein kinases and nitric oxide in human umbilical vein endothelium. *Exp. Physiol.* **2003**, *88*, 209–219.

(3) Lorenzi, M.; Toledo, S.; Boss, G. R.; Lane, M. J.; Montisano, D. F. The polyol pathway and glucose 6-phosphate in human endothelial cells cultured in high glucose concentrations. *Diabetologia* **1987**, *30*, 222–227.

(4) Curcio, F.; Ceriello, A. Decreased cultured endothelial cell proliferation in high glucose medium is reversed by antioxidants: new insights on the pathophysiological mechanisms of diabetic vascular complications. *J. Tissue Cult. Assoc.* **1992**, *28*, 787–790.

(5) Wu, O. D.; Wang, J. H.; Fennessy, F.; Redmond, H. P.; Bouchier-Hayes, D. Taurine prevents high-glucose-induced human vascular endothelial cell apoptosis. *Am. J. Physiol. Cell Physiol.* **1999**, *277*, 1229–1238.

(6) Du, X.; Stockklauser-Farber, K.; Rosen, P. Generation of reactive oxygen intermediates, activation of NF-κB, and induction of apoptosis in human endothelial cells by glucose: role of nitric oxide synthase. *Free Radical Biol. Med.* **1999**, *27*, 752–763.

(7) Suh, K. S.; Nam, Y. H.; Ahn, Y. M.; Kim, N. J.; Park, C. Y.; Koh, G.; Oh, S.; Woo, J. T.; Kim, S. W.; Kim, J. W.; Kim, Y. S. Effect of scutellariae redix extract on the high glucose-induced apoptosis in cultured vascular endothelial cells. *Biol. Pharm. Bull.* **2003**, *26*, 1629–1632.

(8) Baynes, J. W. Role of oxidative stress in development of complications in diabetes. *Diabetes* **1991**, *40*, 405–412.

(9) Bonnefont-Rousselot, D. Glucose and reactive oxygen species. *Cur. Opin. Clin. Nutr. Metab. Care* **2002**, *5*, 561–568.

(10) Wen, Y.; Skidmore, J. C.; Porter-Turner, M. M.; Rea, C. A.; Khokher, M. A.; Singh, B. M. Relationship of glycation, antioxidant status and oxidative stress to vascular endothelial damage in diabetes. *Diabetes Obes. Metab.* **2002**, *4*, 305–308.

(11) Ceriello, A.; Bortolotti, N.; Falleti, E.; Taboga, C.; Tonutti, L.; Crescentini, A.; Motz, E.; Lizzio, S.; Russo, A.; Bartoli, E. Total radical-trapping antioxidant parameter in NIDDM patients. *Diabetes Care* **1997**, *20*, 194–197.

(12) Subramaniam, R.; Fan, X. J.; Scivittaro, V.; Yang, J.; Ha, C. E.; Petersen, C. E.; Surewicz, W. K.; Bhagavan, N. V.; Weiss, M. F.; Monnier, V. M. Cellular oxidant stress and advanced glycation end products of albumin: caveats of the dichlorofluorescein assay. *Arch. Biochem. Biophys.* **2002**, *400*, 15–25.

(13) Yim, H. S.; Kang, S. O.; Hah, Y. C.; Chock, P. B.; Yim, M. B. Free radicals generated during the glycation reaction of amino acids by methylglyoxal. A model study of protein-cross-linked free radicals. *J. Biol. Chem.* **1995**, *270*, 28228–28233.

(14) Li, N.; Karin, M. Is NF-κB the sensor of oxidative stress. *J. Fed. Am. Soc. Exp. Biol.* **1999**, *13*, 1137–1143.

(15) Chen, F. Is NF-κB a culprit in type 2 diabetes. *Biochem. Biophys. Res. Commun.* **2005**, *332*, 1–3.

(16) Srivastava, A. K. Hyperglycemia-induced protein kinase signaling pathways in vascular smooth muscle cells: implications in the pathogenesis of vascular dysfunction in diabetes. *Adv. Exp. Med. Biol.* **2001**, *498*, 311–318.

(17) Brownlee, M. Biochemistry and molecular cell biology of diabetic complications. *Nature* **2001**, *414*, 813–820.

(18) Ceriello, A. New insights on oxidative stress and diabetic complications may lead to a "causal" antioxidant therapy. *Diabetes Care* **2003**, *26*, 1589–1596.

(19) Mullarkey, C. J.; Edelstein, D.; Brownlee, M. Free radical generation by early glycation products: a mechanism for accelerated atherogenesis in diabetes. *Biochem. Biophys. Res. Commun.* **1990**, *173*, 932–939.

(20) Bonnefont-Rousselot, D. Antioxidant and anti-AGE therapeutics: evaluation and perspectives. *J. Soc. Biol.* **2001**, *195*, 391–398.

(21) Iwu, M. M. *Handbook of African Medicinal Plants*; CRC Press: Boca Raton, FL, 1993; pp 223–224.

(22) Lee, H. H. The hypoglycemic effect of *Psidium guajava* L. Master's thesis, Department of Pharmacy, Taiwan University, 1986.

(23) Oliver-Bever, B. *Medicinal Plants in Tropical West Africa*; Cambridge University Press: London, U.K., 1986; p 134.

(24) Hsieh, C. L.; Lin, Y. C.; Ko, W. S.; Peng, C. H.; Huang, C. N.; Peng, R. Y. Inhibitory effect of some selected nutraceutic herbs on LDL glycation induced by glucose and glyoxal. *J. Ethnopharmacol.* **2005**, *102*, 357–363.

(25) La Torre, G. L.; Saitta, M.; Vilasi, F.; Pellicano′, T.; Dugo, G. Direct determination of phenolic compounds in Sicilian wines by liquid chromatography with PDA and MS detection. *Food Chem.* **2006**, *94*, 640–650.

(26) Mossmann, T. Rapid colorimetric assay for cellular growth and survival: application to proliferation and cytotoxicity assays. *J. Immunol. Methods* **1983**, *65*, 55–63.

(27) Takada, E.; Toyota, H.; Suzuki, J.; Mizuguchi, J. Prevention of anti-IgM induced apoptosis accompanying G1 arrest in B lymphoma cells overexpressing dominant-negative mutant form of c-Jun N-terminal kinase. *J. Immunol.* **2001**, *166*, 1641–1649.

(28) Pan, M. H.; Liang, Y. C.; Lin-Shiau, S. Y.; Zhu, N. Q.; Ho, C. T.; Lin, J. K. Induction of apoptosis by the Oolong tea polyphenol theasinensin a through cytochrome *c* release and activation of caspase-9 and caspase-3 in human U937 cells. *J. Agric. Food Chem.* **2000**, *48*, 6337–6346.

(29) Eu, J. P.; Liu, L.; Zeng, M.; Stamler, J. S. An apoptotic model for nitrosative stress. *Biochemistry* **2000**, *39*, 1040–1047.

(30) Hagerman, A. E.; Riedl, K. M.; Alexander, J. G.; Sovik, K. N.; Ritchard, N. T.; Hartzfeld, P. W.; Riechel, T. L. High molecular weight plant polyphenolics (tannins as biological antioxidant). *J. Agric. Food Chem.* **1998**, *46*, 1887–1892.

(31) Bae, J. W.; Lee, M. H. Effect and putative mechanism of action of ginseng on the formation of glycated hemoglobin in vitro. *J. Ethnopharmacol.* **2004**, *91*, 137–140.

(32) Coskun, O.; Kanter, M.; Korkmaz, A.; Oter, S. Quercetin, a flavonoid antioxidant, prevents and protects streptozotocin-induced oxidative stress and β-cell damage in rat pancreas. *Pharmacol. Res.* **2005**, *51*, 117–123.

(33) Anjaneyulu, M.; Chopra, K. Quercetin, a bioflavonoid, attenuates thermal hyperalgesia in a mouse model of diabetic neuropathic pain. *Prog. Neuropsychopharmacol. Biol. Psych.* **2003**, *27*, 1001–1005.

(34) Bousova, I.; Bakala, H.; Chudacek, R.; Palicka, V.; Drsata, J. Glycation-induced inactivation of aspartate aminotransferase, effect of uric acid. *Mol. Cell Biochem.* **2005**, *278*, 85–92.

(35) Nakagawa, T.; Yokozawa, T.; Terasawa, K.; Shu, S.; Juneja, L. R. Protective activity of green tea against free radical- and glucose-mediated protein damage. *J. Agric. Food Chem.* **2002**, *50*, 2418–2422.

(36) Bassi, A. M.; Ledda, S.; Vaslentini, S.; De Pascale, M. C.; Rossi, S. Damaging effects of advanced glycation end-products in the murine macrophage cell line J774A.1. *Toxicol. In Vitro* **2002**, *16*, 339–347.

(37) Danga, L.; Sealeb, J. P.; Qua, X. Reduction of high glucose and phorbol-myristate-acetate-induced endothelial cell permeability by protein kinase C inhibitors LY379196 and hypocrellin A. *Biochem. Pharmacol.* **2004**, *67*, 855–864.

(38) Shimoi, K.; Okitsu, A.; Green, M. H. L.; Lowe, J. E.; Ohta, T.; Kaji, K.; Terato, H.; Ide, H.; Kinae, N. Oxidative DNA damage induced by high glucose and its suppression in human umbilical vein endothelial cells. *Mutat. Res.* **2001**, *480–481*, 371–378.

(39) Wondrak, G. T.; Cervantes-Laurean, D.; Roberts, M. J.; Qasem, J. G.; Kim, M.; Jacobson, E. L.; Jacobson, M. K. Identification of α-dicarbonyl scavengers for cellular protection against carbonyl stress. *Biochem. Pharmacol.* **2002**, *63*, 361–373.

(40) Dent, P.; Grant, S. Pharamacologic interruption of mitogen-activated extracellular-regulated kinase/mitogen-activated protein kinase signal transduction pathway: potential role in promoting cytotoxic drug action. *Clin. Cancer. Res.* **2001**, *7*, 775–783.

(41) Takaishi, H.; Taniguchi, T.; Takahashi, A.; Ishikawa, Y.; Yokoyama, M. High glucose accelerates MCP-1 production via p38 MAPK in vascular endothelial cells. *Biochem. Biophys. Res. Commun.* **2003**, *305*, 122–128.

(42) Ceriello, A. Postprandial hyperglycemia and diabetes complications. *Diabetes* **2005**, *54*, 1–7.

Received for review June 23, 2007. Revised manuscript received August 23, 2007. Accepted August 28, 2007. This research work was supported by the National Science Council, Republic of China (Grant NSC 94-2313-B-241-006).

JF071858B